Available online at www.sciencedirect.com
ScienceDirect
Catalysis Today 133–135 (2008) 374–382
CATALYSIS TODAY
www.elsevier.com/locate/cattod

Study of the composition of ternary mixed oxides: Use of these materials on a hydrogen production process

F. Melo *, N. Morlanés

Instituto de Tecnología Química, UPV-CSIC, Avda. los Naranjos s/n, 46022 Valencia, Spain

Available online 1 February 2008

Abstract

Mixed oxides obtained by thermal decomposition of layered double hydroxides have been studied in the reaction of hydrocarbon steam reforming for producing hydrogen. The introduction of several elements on the structure could influence the metal electronic configuration, reducibility, particle size, dispersion and surface area modifying its catalytic performance. The effect of composition on structure and reactivity of these materials has been studied. Nickel, magnesium and aluminium from base catalyst have been substituted by different elements. Ni has been substituted by other active metals for this process like Co, Cu, Pd or Ru; Mg has been substituted by Mn, Zn, Ca or Li; and Al has been substituted by Fe, Cr, La or Ce. Samples have been characterized by N_2 adsorption (BET), X-ray diffraction (XRD), temperature-programmed reduction (TPR) and elemental analysis. Composition has an important effect on catalytic performance.

Keywords: Steam reforming; Mixed oxides; Nickel catalysts promotion

1. Introduction

As a source of energy, fossil fuels produce huge impact over the planet in different ways, including human safety and the environment. In order to solve the associated problem with the use of petroleum as a source of energy, scientists are investigating methods to improve the yield of energy with a minimum level of toxic effluents [1]. In the last few years, extensive literature with different options for cleaner energy sources, their advantages, handicaps and economic aspects has appeared, and there is a common statement: in the long term hydrogen seems to be the most suitable large-scale fuel because it has several advantages like its clean combustion (only produces energy and water), allowing generation from any imaginable source of energy and the possibility of storage over time [2]. Thus, hydrogen offers a potentially non-polluting and efficient fuel for today's rising energy demands.

The advantages of using hydrogen as fuel, in terms of greenhouse gases emission, will depend on how it is produced [3]. In the long term, a hydrogen-based energy system would have to use renewable primary energy sources for meeting sustainability goals. Reaching this scenario will require a significant cost and performance improvements in production, conversion, storage, transportation, distribution and end-use technologies. The transition to a fully developed "hydrogen economy" will need structural changes, which will span over many decades [4].

In the near and mid-term, hydrogen production from hydrocarbons seems to be the best option to achieve a gradual transition, because we can use actual infrastructure. The alternative to the lack of hydrogen refuelling infrastructure and the low density of hydrogen storage is to carry liquid fuels that have high energy density and convert them to hydrogen-rich gases via fuel processing using different techniques [5,6]. In the presence of catalysts, fuels can be reformed through partial oxidation, steam reforming, or autothermal reforming to generate hydrogen. The gases produced by steam reforming contain up to 70% hydrogen, whereas those obtained by partial oxidation or autothermal reforming have lower hydrogen content (35–45%) [6].

Hydrocarbon steam reforming process, is performed at high temperature and low pressure over Ni-based catalysts. However, the high temperature required may favour several routes to the formation of carbon deposits such as the Boudouard reaction and methane/hydrocarbon decomposition. Additionally, Ni catalysts tend to agglomerate and then lose

* Corresponding author.
E-mail address: fmelo@itq.upv.es (F. Melo).

0920-5861/$ – see front matter © 2007 Elsevier B.V. All rights reserved.
doi:10.1016/j.cattod.2007.12.059

their active surface area under steam reforming conditions, resulting in short catalyst lifetimes [7–11]. Although coke formation is a major concern for Ni-based catalysts when are used for hydrocarbon steam reforming, their low cost and long-proven performance warrant further investigation.

Key challenges for development of novel catalytic systems include carbonaceous deposit formation particularly at lower steam/carbon ratios, short lifetimes due to loss of active surface area and metal agglomeration under steam reforming conditions, sulphur tolerance, and resistance to other poisons found in the feed stream. Current research focuses on synthesis, formulation and characterization of catalysts designed to meet these challenges [12]. Solving the hydrogen generation problems will ultimately help drive advancements in fuel cell technology, which brings a hydrogen energy future much closer to reality.

Intensive research is needed to improve catalytic processes and uncover new generation of catalysts with higher activity, more resistance to coke deposition and higher ability to reform gasoline and diesel fuels at lower temperatures. In this light, development of nanocatalysts (ultrafine particles of metals, metal oxides and composites), which are supposed to have higher surface area than conventional catalysts, and thereby higher activity, will lead to cost-effective reforming processes.

Layered double hydroxides (LDHs), or hydrotalcite-like (HT) compounds with general formula $[M^{2+}_{1-x}M^{3+}_{x}(OH)_2]^{x+}[A_{x/n}]^{n-}\cdot mH_2O$, are lamellar materials of Brucite-like layers with positive charge and anionic compounds in the interlayer to form neutral compounds which possess versatile acid–basic and redox properties and have potential applications in various catalytic fields [13–15]. These materials may contain divalent (M^{2+}) and trivalent (M^{3+}) cations then various kinds of transition metals could be introduced into the Brucite-like layer having a high potential function as the catalytic active centre. LDH compounds easily decompose after calcinations, into a mixed oxide of the $M^{2+}M^{3+}(O^{2-})$ type. Further reduction of LDH compounds or mixed oxides, containing reducible cation yields supported metal catalysts [16,17]. Catalysts obtained by calcination/reduction of hydrotalcite-type materials are characterized by highly dispersed metallic crystallites stabilized inside a matrix with high surface area.

In a previous work [18] we have studied LDH-based catalysts (NiMgAl), and they show higher activity than do conventional supported catalysts due to the higher BET and metal areas, higher metal dispersions and smaller nickel particle size. Other studies have been realized using these materials in reforming reactions [19,20]. In another work synthesis parameters like nickel content, Al/Mg ratio, calcination and reduction temperature and method of nickel introduction on the structure have been studied along with the influence of these parameters on structure and reactivity of these materials in the mentioned reaction. Synthesis parameters such as method of introduction of active species, amount of components and thermal treatments (calcinations and reduction), could be optimized to obtain a material which presents high catalytic activity and high resistance to carbon formation.

Thus, rational design of adaptable multifunctional nanostructured catalysts based on LDH precursors becomes a real possibility which offers the opportunity of controlling the nature of the active sites and their environment, the texture and the stability of the catalysts. Due to their wide variety of compositions, LDHs are attractive precursors of multicomponent nanostructured catalysts, highly functionalized at atomic level [21,22].

In order to develop an efficient liquid hydrocarbon steam reforming catalyst, in the present work, we have studied the influence of the composition of LDH compound-derived catalysts, on the structure and reactivity of these materials on hydrocarbon steam reforming. This work reports synthesis, physicochemical characterization and catalytic testing of three-element mixed oxides obtained by precipitation method of LDH compounds with different composition. Nickel, magnesium and aluminium from base catalyst studied in a previous work, have been substituted by different elements. Ni has been substituted by other active metals for this process like Co, Cu, Pd or Ru; Mg has been substituted by Mn, Zn, Ca or Li; and Al has been substituted by Fe, Cr, La or Ce.

2. Experimental

2.1. Catalysts synthesis

Several materials LDH type have been prepared by the coprecipitation method, constituted by the following steps: materials type HT-Ni/Mg/Al: it has been synthesized several LDHs with nickel in the structure maintaining the relation $R = [Al^{3+}/(Ni^{2+} + Mg^{2+} + Al^{3+})] = 0.25$. For the synthesis of these materials two solutions are prepared [23]; an acid and another basic one. The acid solution contains nitrates of magnesium, nickel and aluminium with a total concentration $(Ni^{2+} + Mg^{2+} + Al^{3+}) = 1.5$ M and the established relation R. Whereas the basic solution is obtained mixing suitable amounts of NaOH with Na_2CO_3 that allow to maintain the relation $[CO_3^{2-}/(Ni^{2+} + Mg^{2+} + Al^{3+})] = 0.66$ and pH of synthesis in 13. Solutions are added simultaneously into a bottle, and the following parameters have been fixed: addition speed is 20 ml/h, room temperature, atmospheric pressure and with vigorous mechanical agitation during 4 h. The obtained gel ages in propylene boats at 333 K during 12 h, after the aging the solid is filtered and washed with distilled water until the pH reaches neutral value (pH 7) and carbonates are not detected. Finally, the LDH material is dried at 333 K during 14 h and is calcined in air up to 923 K during 6 h obtaining a mixed oxide Ni/Mg/Al. Supported metal catalysts suitable for steam reforming reaction are obtained from these precursors after reduction step. The activation of the materials is realized with a mixture 20% molar H_2 on N_2 to 1073 K during 1 h.

Materials type HT-M^{2+}/Mg/Al: These materials were synthesized following the same procedure described in the preparation of the HT-Ni/Mg/Al materials, but replacing nickel nitrates by another cation nitrate like ruthenium, palladium, cupper and cobalt (Ru, Pd, Cu, Co).

Materials type HT-Ni/M^{2+}/Al: These materials were synthesized following the same procedure described in the preparation of the HT-Ni/Mg/Al materials, but replacing magnesium nitrates

by nitrates of other cations like manganese, calcium, zinc and lithium (Mn, Ca, Zn, Li). In the case of the sample with lithium, it comes from a LDH with chemical composition $[Al_2Li(OH)_6]$-$CO_3 \cdot nH_2O$, that has been prepared by hydrothermal synthesis from aluminium tri-sec-but oxide carbonate and lithium carbonate [23]. Organic solution has been prepared with hexane containing aluminium tri-sec-but oxide carbonate. Aqueous solution has been prepared with lithium carbonate. Solutions are mixed by the slow addition of the organic one above the aqueous one, with constant agitation and ambient temperature. Final pH of the gel is 10. Gel aging, calcination and reduction steps are the same as for materials type HT-Ni/Mg/Al.

Materials type HT-Ni/Mg/M^{3+}: These materials were synthesized following the same procedure described in the preparation of the HT-Ni/Mg/Al materials, but replacing aluminium nitrates by nitrates of trivalent cations like chromium, iron, lanthanum and cerium (Cr, Fe, La, Ce).

2.2. Catalysts characterization

The obtained materials (calcined, reduced and used for catalytic measurements samples) have been characterized by several techniques in order to correlate catalytic activity results with their structural properties.

Chemical composition of calcined samples was determined by atomic absorption spectrophotometry using a Varian Spectra A-10 Plus apparatus. Samples were first dissolved in acid solutions (a mixture of HCl and HNO_3), and diluted to concentrations within the detection range of the instrument.

N_2 adsorption isotherms were obtained for calcined samples at 77 K over the whole range of relative pressures, using a Micromeritics ASAP 2000 automatic device on samples previously outgassed at 423 K for 12 h. BET specific areas were calculated from these isotherms using the BET method.

X-ray powder diffractograms were recorded for calcined, reduced and used samples, following the step-scanning procedure (step size 0.02°, 2θ scanning from 5° to 70°) using a Phillips X'pert diffractometer (monochromatized Cu Kα radiation, $\lambda = 0.15418$ nm). The average particle size for different phases present on each state of the sample (calcined, reduced or used) were estimated by Scherrer equation [24] using the most intense reflexion (nickel oxide: $2\theta = 43.3°$ of calcined samples diffractograms, and metallic nickel: $2\theta = 51°$ of reduced samples diffractograms).

Nickel area has been estimated by means of a proposed equation on literature [25] that considers nickel particle size, nickel content on the sample and reduction degree reached on the activation stage. The equation is the following one:

$$A_{Ni} = \frac{5 \times 10^4 X_{Ni} \alpha_{Ni}}{\gamma_{Ni} d_{Ni}} \quad (1)$$

where A_{Ni}: nickel active area (m^2/g_{cat}); X_{Ni}: nickel content of the sample (g_{Ni}/g_{cat} %); α_{Ni}: reached reduction degree ($g_{Ni}{}^{\circ}/g_{Ni}$ %); γ_{Ni}: nickel specific density, 8.9 g/cm^3; d_{Ni}: nickel particle size (Å); 5×10^4: geometric factor taking into account nickel particle geometry.

Ni^0 metal dispersions can be estimated using another equation proposed on the literature [26], which has into account Ni^0 particle size and assumes spherical geometry of the metal particles with uniform site density. The equation is the following one:

$$D(\%) = \frac{971}{d_{Ni}(\text{Å})} \quad (2)$$

The reducibility of the calcined samples was studied by temperature-programmed reduction in Micromeritics Autochem 2910 equipment, using a thermal conductivity detector in order to determine H_2 consumption. From temperature-programmed reduction curves, temperature at which a maximum in the curve appears (nickel reduction temperature), has been used like a nickel-support interaction degree measurement, being it more intense when temperature is higher. Reduction degree has been estimated comparing temperature-programmed reduction curves corresponding to calcined and reduced samples.

Coke formation on samples during activity tests has been determined by elemental analysis in an Elemental Analizer CE1110, model CHNS.

2.3. Catalytic activity measurements

Steam reforming reaction study is carried out in a down-flow fixed-bed catalytic system designed for this purpose, which allows to compare different catalysts and reaction conditions, with the aim of optimising hydrogen production.

Hydrocarbon feed is composed of a mixture of *n*-heptane and *n*-hexane (in a weight ratio $C_7/C_6 = 2$) simulating a naphtha. Water and hydrocarbon feed are introduced, mixed with a proportion of nitrogen and hydrogen. Nitrogen is used as carrier gas and as internal pattern for gas analysis. Hydrogen is used to avoid nickel oxidation on reduced samples. Molar proportion of the reactant mixture is hydrocarbon/H_2O/H_2/N_2: 2/40/5/53.

Activity tests were performed using 0.5 g of catalyst (0.25–0.42 mm particle size) diluted with SiC (0.42–0.60 mm particle size) at a volume ratio of 10:1 to avoid adverse thermal effects.

The samples in their reduced form are tested in the naphtha steam reforming process. Operation conditions studied are: $P = P_{atm}$, $T = 673$–1073 K, S/C = 3 H_2O mol/atom C, W/F = 5.8 g_{cat} h/hydrocarbon mol, G_{total} HSV = 112,580 h^{-1}.

The catalyst bed is placed in a stainless-steel reactor ($d_i = 10$ mm, $l = 400$ mm) with several coaxially centred thermocouples. During the reaction the temperature in the catalyst bed is maintained and controlled by means of three independent heating zones with the corresponding temperature controllers.

The reaction products are analysed on-line by gas chromatography. The gas chromatograph is constituted by two independent channels, equipped each one of them with a thermal conductivity detector. First channel allows to separate CO_2, CO, CH_4 and N_2; and the second one allows separate hydrogen from the rest of constituents.

In order to compare catalytic activity for different catalysts, several tests have been made at the same operation conditions (pressure, steam/carbon ratio and contact time) and varying reaction temperature. We have compared hydrocarbon conversion as a function of reaction temperature, therefore the most active catalyst is that which allows to reach the greatest conversion degree at the same temperature of reaction. In this case the activity measurement used to compare the behaviour for different catalysts corresponds to conversion after an hour on stream for each temperature.

In order to compare catalyst resistance to carbon deposition we have compared the carbon content present on used samples analysed by elemental analysis of different samples exposed to the same reaction conditions.

We have studied hydrocarbon conversion and carbon deposition resistance as catalytic characteristics presented by these materials, since selectivity to different products is determined by thermodynamic equilibrium between gaseous species according to operation conditions at which this process takes place (pressure, temperature, steam/carbon ratio and space velocity) and it was studied in a previous work [18].

3. Results and discussion

Hydrocarbon steam reforming is an important process for hydrogen production. Steam reforming process transforms a liquid hydrocarbon stream into a gaseous mixture constituted by CO_2, CO, CH_4 and H_2 [6–8]. The main reactions that take place are the following ones:

$$C_nH_m + nH_2O \rightarrow nCO + (n + 1/2\,m)H_2 \qquad \Delta H > 0 \qquad (3)$$

$$CO + 3H_2 \leftrightarrow CH_4 + H_2O \qquad \Delta H = -206\,kJ/mol \qquad (4)$$

$$CO + H_2O \leftrightarrow CO_2 + H_2 \qquad \Delta H = -41.2\,kJ/mol \qquad (5)$$

In order to correlate activity results with structural characteristics of the catalysts we must take into account several mechanism considerations. Reaction mechanism, proposed by Rostrup Nielsen, establishes that hydrocarbon molecules are adsorbed on a dual site on catalyst surface where nickel selectively attacks terminal carbon of the chain by means of successive α-scission steps. The C_1 species formed can react with oxygen species coming from water adsorption–dissociation, or remain adsorbed on the active sites where they would be transformed according to one of the possible carbon formation routes. We can outline this sequence

hydrocarbon adsorption is separated Hydrocarbon adsorption−

$$\text{dissociation}: \quad C_nH_m + 2* \rightarrow C_nH_z - - *2 + (m - z)/2H2 \qquad (6)$$

$$C-C\alpha\text{-scission}: \quad C_nH_z - - *2 + n* \rightarrow C_{n-1}H_z' - - *2 + CH_x - - *n \qquad (7)$$

Steam adsorption is separated Steam adsorption−

$$\text{dissociation}: \quad H_2O + \text{support} \rightarrow H_2O - - \text{support} \qquad (8)$$

$$H_2O - - \text{support} + * \rightarrow O - - * + H2 + \text{support} \qquad (9)$$

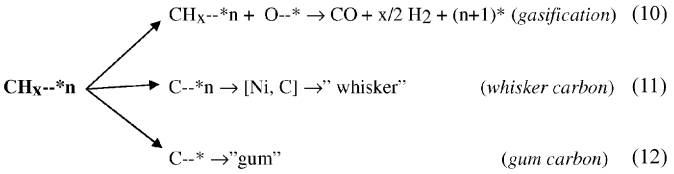

*: represents active sites, *2: represents adsorption sites acting at the same time.

Steam reforming reaction takes place on the surface of a solid catalyst. For this process usually nickel-supported catalysts are used. Water adsorbs preferentially on the catalysts support, formulated to allow mobility for oxygen species (which proceed from water dissociation) adsorbed on its surface, hydrocarbon molecules adsorb preferentially on the metal surface (metallic nickel), and the steam reforming reaction takes place at the metal support interface [7]. Therefore, the most important factors related to the catalysts structure influencing the activity of a steam reforming catalyst are metal area, metal particle size, support area and its ability to adsorb water and metal–support interface.

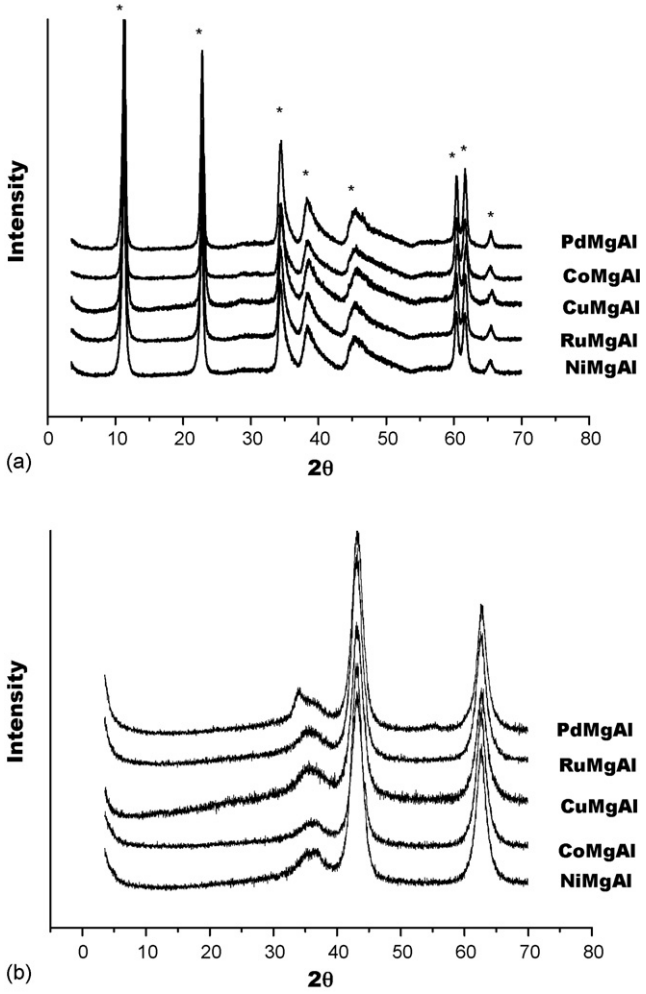

Fig. 1. X-ray diffraction diagrams samples type HT-M^{2+}/Mg/Al. a) Before calcination stage, *: $[M^{2+}_{1-x}M^{3+}_{x}(OH)_2]^{x+}[A_{x/n}]^{n-}\cdot mH_2O$ b) after calcination stage, +: mixed oxide.

Table 1
Characterization samples type HT-M^{2+}/Mg/Al

Sample	Percentage in weight (%)				Molar ratio			BET area (m^2/g_{cat})
	M(II)	Mg	Al	O	Al	Mg	M(II)	
NiMgAl	5.1	37.5	14.6	42.7	25.0	71.0	4.0	229
CuMgAl	4.9	38.4	14.9	41.8	25.0	71.5	3.5	222
CoMgAl	5.1	39.9	15.5	39.5	25.0	71.2	3.8	233
PdMgAl	1.0	41.9	15.5	41.6	25.0	74.6	0.4	218
RuMgAl	0.9	37.7	14.0	47.4	25.0	74.6	0.4	201

3.1. Nickel substitution

Nickel from NiMgAl base material has been replaced by other active metals like Co, Cu, Pd or Ru to determine the activity for other metals in the hydrocarbon steam reforming process.

In Fig. 1a we can see the diffraction diagrams of X-rays corresponding to the synthesized materials previous to the calcination stage, in this figure we can see that all the samples show LDH structure. After calcination stage this material decomposes into an amorphous mixed oxide (Fig. 1b) with a mesoporous surface and elevated specific area as we can see in Table 1. In this table appears the composition of the synthesized materials, with 5% of nickel in weight, Cu or Co, and 1% in weight of Pd or Ru and the rest is Mg and Al always maintaining the relation Al/(Al + Mg + M) = 0.25.

In Fig. 2 we can see curves of temperature-programmed reduction corresponding to the synthesized materials. In this figure we can see that Ni and Co are the metals which are more difficult to reduce, whereas the Cu, Ru and mainly the Pd (that presents a small reduction signal at, practically, ambient temperature) are reduced at much more low temperature, indicating that the interaction of these elements with the MgAl support is much smaller.

Finally in Fig. 3 is shown the catalytic behaviour of these materials in naphtha steam reforming process. The sample of NiMgAl is the most active in all range of temperatures studied and also is the most resistant to coke formation with the exception of PdMgAl and RuMgAl samples that, are based on noble metal that do not dissolve carbon [27], so they present a minor carbon content after the reaction.

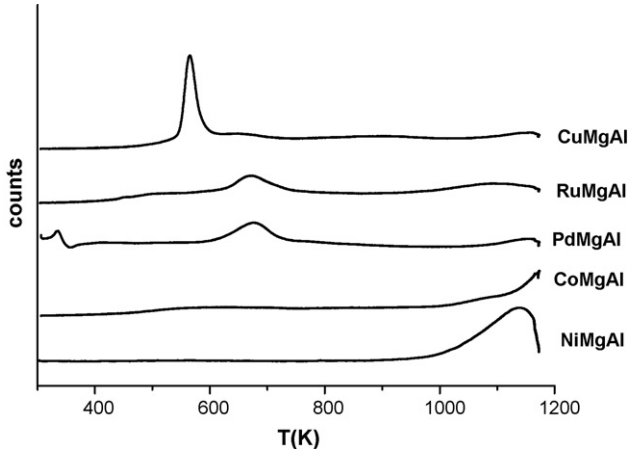

Fig. 2. Curves of temperature-programmed reduction, samples type HT-M^{2+}/Mg/Al.

3.2. Magnesium substitution

Magnesium from NiMgAl base material has been replaced by Mn, Zn, Ca or Li, to study the influence of other elements on intrinsic activity of nickel in the hydrocarbon steam reforming process.

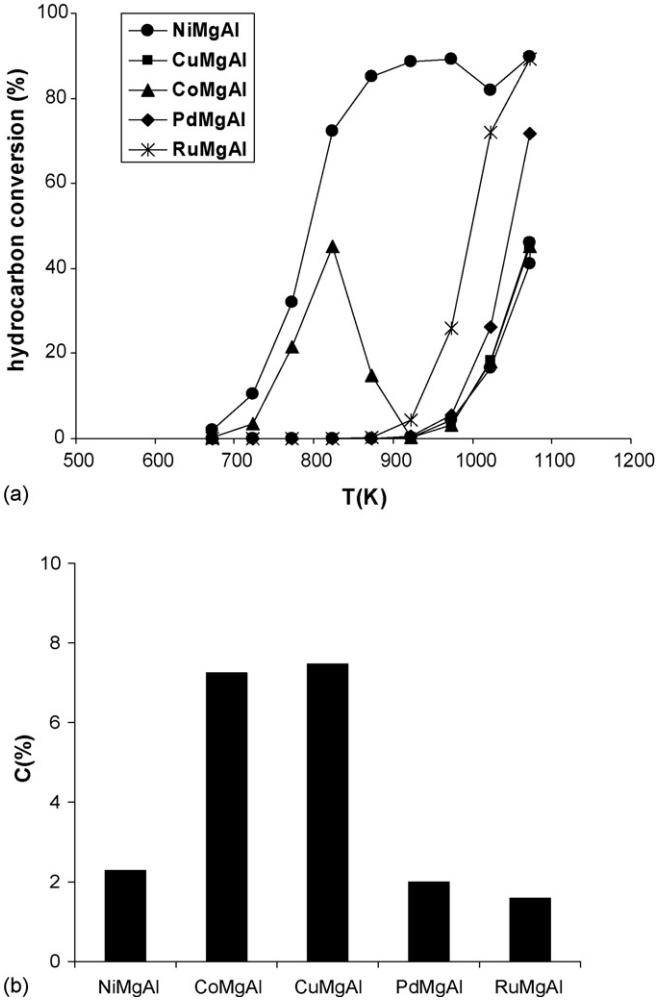

Fig. 3. (a) Hydrocarbon conversion; (b) carbon content, samples type HT-M^{2+}/Mg/Al ($P = P_{atm}$, T = 673–1073 K, S/C = 3 H_2O mol/C atom, W/F = 5.8 g_{cat} h/hydrocarbon mol, G_{total} HSV = 112,580 h^{-1}).

Table 2
Characterization samples type HT-Ni/M^{2+}/Al

Sample	Percentage in weight (%)				Molar ratio		
	Ni	M(II)	Al	O	Al	M(II)	Ni
NiMgAl	10.2	35.4	14.6	39.8	25.0	67.2	7.8
NiCaAl	9.9	45.8	11.8	32.5	25.0	65.4	9.6
NiMnAl	10.1	53.3	10.2	26.4	25.0	63.7	11.3
NiZnAl	9.7	54.4	8.9	26.9	25.0	62.6	12.4
NiLiAl	9.8	14.4	20.1	55.7	25.0	69.4	5.6

Reduced samples characterization

Sample	BET area (m^2/g_{cat})	d_{Ni} (nm)	Dispersion (%)	Active area (m^2_{Ni}/g_{cat})
NiMgAl	241	13	7.8	4.4
NiCaAl	28	57	1.7	0.9
NiMnAl	121	42	2.3	1.3
NiZnAl	135	10	9.6	5.4
NiLiAl	87	62	1.6	0.9

In Table 2 appears the composition of these materials synthesized with 10 wt.% of nickel and the rest is constituted by the element that replaces Mg, M and Al always maintaining the relation Al/(Al + M + Ni) = 0.25.

In Fig. 4a we can see the diffraction diagrams of X-rays corresponding to the synthesized materials previous to the calcination stage, all the samples show LDH structure, except NiCaAl and NiZnAl samples that, in addition to these signals of diffraction, present diffraction signals corresponding to other segregated phases.

Fig. 4b presents diffraction diagrams corresponding to the samples prepared after the calcination stage. Peak widths would correlate with crystalline particle size, and we can see that NiMgAl sample presents the slowest particle size and therefore the greatest specific surface area, then we can verify it in Table 2. In this table we can also observe the characterization correspondent to reduced samples, NiZnAl and NiMgAl samples present greater active surface, greater dispersion of nickel and lower nickel particle size than the rest of the samples.

In Fig. 5 we can see curves of temperature-programmed reduction corresponding to the synthesized materials. In this figure we observe that the reduction of nickel moves towards lower temperatures with respect to the NiMgAl sample when replacing Mg by other elements. NiMnAl sample also presents signals of reduction corresponding to possible changes of the oxidation state for Mn. The presence of oxides more easily reducible than nickel oxide facilitates the process of reduction of the sample, whereas the presence of oxides more hardly reducible slows down the process [28–30].

Finally in Fig. 6 is shown the catalytic behaviour of these materials in naphtha steam reforming process. NiLiAl sample is the most active in all range of temperatures studied and also is the most resistant to carbon formation, in spite of being a sample with minor specific area and smaller nickel active area than NiMgAl or NiZnAl samples. The presence of lithium on mixed oxide has greater basicity than magnesium mixed oxide, which is associated to the more electropositive character of

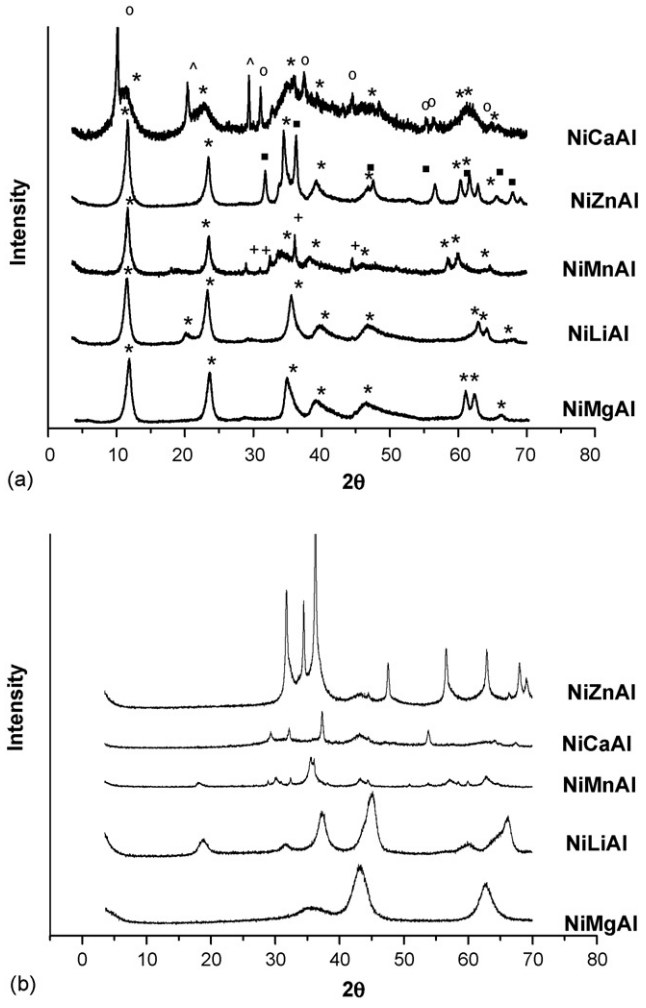

Fig. 4. X-ray diffraction diagrams samples type HT-Ni/M^{2+}/**Al**. a) Before calcination stage, *: $[M^{2+}_{1-x}\ M^{3+}_{x}\ (OH)_2]^{x+}\ [A_{x/n}]^{n-}{\cdot}mH_2O$, o: $Ca_2Al(OH)_7{\cdot}13H_2O$, ^: $CaCO_3{\cdot}H_2O$, +: Mn_2O_3, ·: ZnO b) after calcination stage, +: mixed oxide.

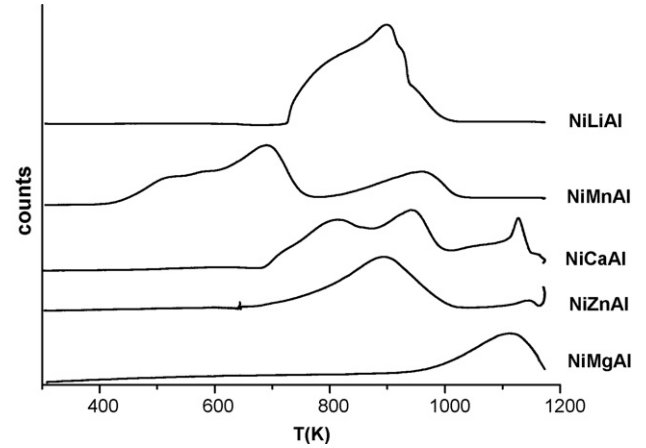

Fig. 5. Curves of temperature-programmed reduction, samples type HT-Ni/M^{2+}/Al.

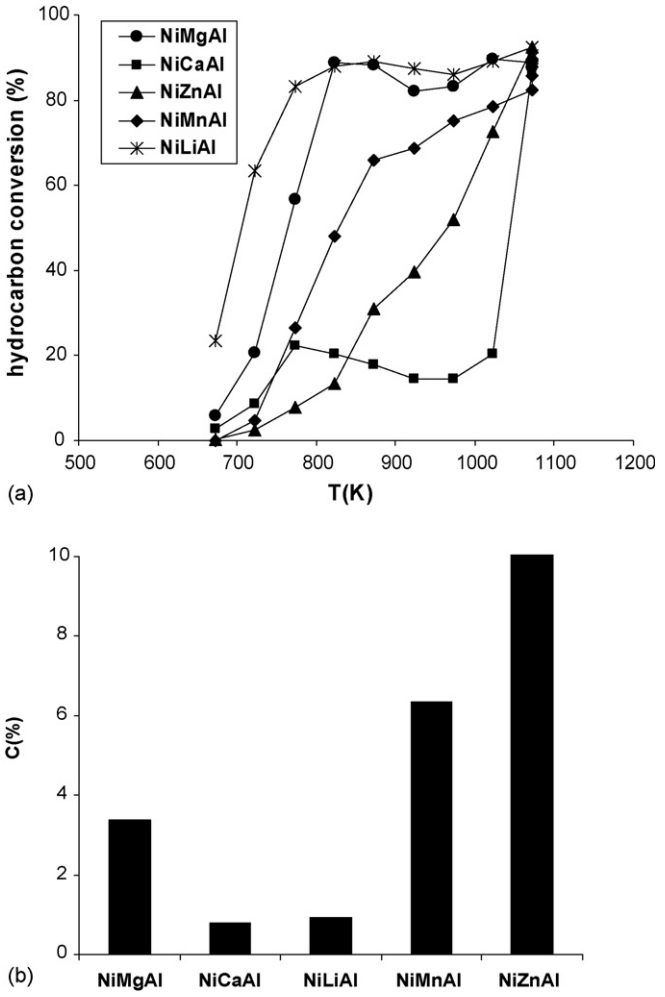

Fig. 6. (a) Hydrocarbon conversion; (b) carbon content, samples type HT-Ni/M^{2+}/Al ($P = P_{atm}$, $T = 673–1073$ K, S/C = 3 H_2O mol/C atom, W/F = 5.8 g_{cat} h/hydrocarbon mol, G_{total} HSV = 112,580 h^{-1}).

lithium with respect to the magnesium, producing the existence of basic centres (O^{2-} species) with greater negative density charge than magnesium oxide, and therefore more strong [23]. Therefore, high surface area and high metallic active area are not sufficient to obtain the greatest activity, it has been shown that the composition of the surroundings of nickel also influences its intrinsic activity.

3.3. Aluminium substitution

Aluminium from NiMgAl base material has been replaced by Cr, Fe, La or Ce to study the influence of other elements on intrinsic activity of nickel in the hydrocarbon steam reforming process.

In Table 3 appears the composition of these materials synthesized with a 10 wt.% of nickel and the rest constituted by Mg and the element that replaces Al, M, always maintaining the relation M/(M + Mg + Ni) = 0.25.

In Fig. 7a we can observe the diffraction diagrams of X-rays corresponding to the synthesized materials previous to the calcination stage, all the samples present LDH structure, except

Table 3
Characterization samples type HT-Ni/Mg/M^{3+}

Sample	Percentage in weight (%)				Molar ratio		
	Ni	Mg	M(III)	O	M(III)	Mg	Ni
NiMgAl	10.2	35.4	14.6	39.8	25.0	67.2	7.8
NiMgCe	10.1	20.1	46.7	23.0	25.0	62.1	12.9
NiMgLa	10.2	20.4	47.0	22.4	25.0	62.2	12.8
NiMgCr	9.8	30.1	24.4	35.7	25.0	66.1	8.9
NiMgFe	9.9	29.7	25.9	34.4	25.0	65.9	9.1

Reduced samples characterization

Sample	BET area (m_2/g_{cat})	d_{Ni} (nm)	Dispersion (%)	Active area ($m^2{}_{Ni}/g_{cat}$)
NiMgAl	241	13	7.8	4.4
NiMgCe	108	108	0.9	0.5
NiMgLa	62	116	0.8	0.5
NiMgCr	43	103	0.9	0.5
NiMgFe	68	139	0.7	0.4

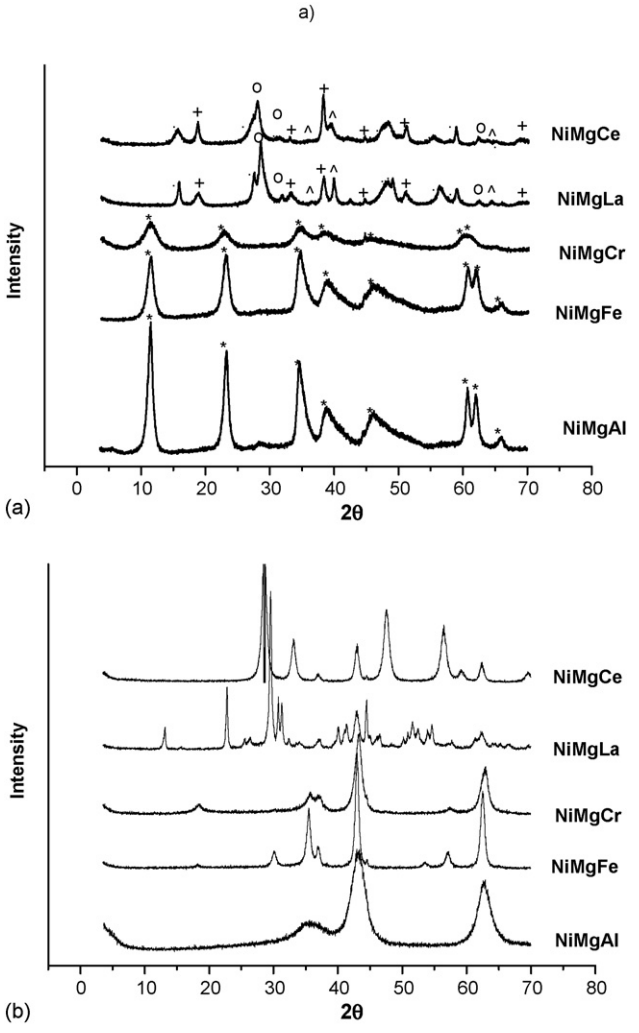

Fig. 7. X-ray diffraction diagrams samples type HT-Ni/Mg/M^{3+}. a) Before calcination stage, *: $[M^{2+}{}_{1-x}\ M^{3+}{}_{x}\ (OH)_2]^{x+}\ [A_{x/n}]^{n-}{\cdot}mH_2O$, o: L_2NiO, ^: L_2MgO, +: $Mg(OH)_2$, ·: $L(OH)_3$, L = La or Ce; b) after calcination stage, +: mixed oxide.

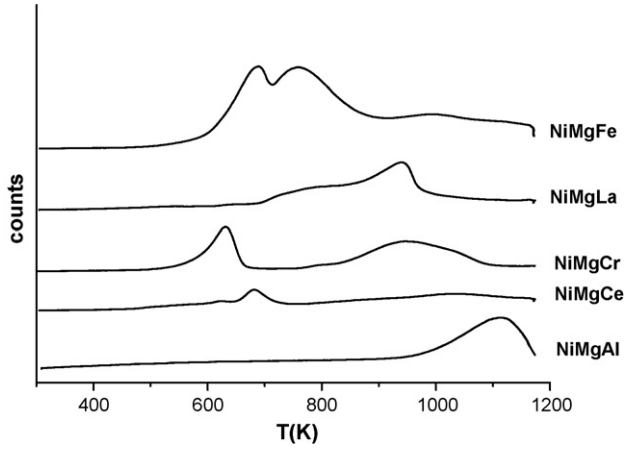

Fig. 8. Curves of temperature-programmed reduction, samples type HT-Ni/Mg/M^{3+}.

NiMgLa and NiMgCe samples in which La and Ce cations cannot be introduced in the cationic layers that constitute LDH structure, since its size is much greater [31,32]; NiMgCr sample presents signals of diffraction with the smallest intensity indicating low crystallinity for the structure.

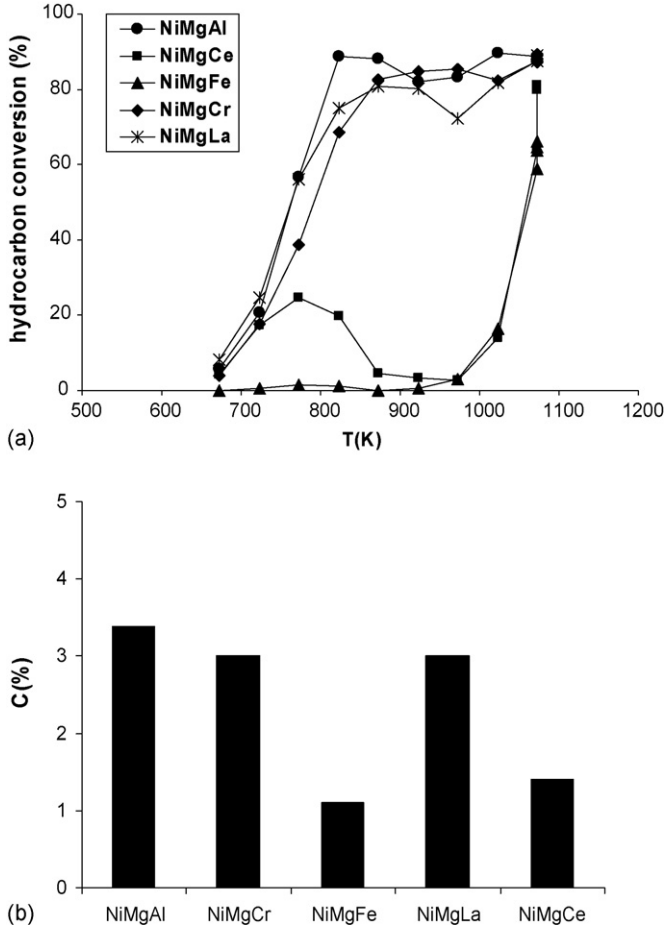

Fig. 9. (a) Hydrocarbon conversion; (b) carbon content, samples type HT-Ni/Mg/M^{3+} ($P = P_{atm}$, T = 673–1073 K, S/C = 3 H_2O mol/C atom, W/F = 5.8 g_{cat} h/hydrocarbon mol, G_{total} HSV = 112,580 h^{-1}).

Fig. 7b presents the diagrams of diffraction corresponding to the samples prepared after the calcination stage. Peaks width would correlate with crystalline particle size, and we can see that NiMgAl sample presents the slowest particle size and therefore the greatest specific surface area, then we can verify it in Table 3. In this table we can also observe characterization correspondent to reduced samples, NiMgAl sample presents greater active surface, greater dispersion of nickel and lower nickel particle size than the rest of the samples.

In Fig. 8 we can see curves of temperature-programmed reduction corresponding to the synthesized materials. In this figure we can observe that the reduction of nickel moves towards lower temperatures with respect to NiMgAl sample when replacing Al by other elements. NiMgCr, NiMgFe and NiMgCe samples also present signals of reduction corresponding to possible changes in oxidation state for Cr, Fe and Ce, respectively, in addition to the signal of nickel reduction.

Finally in Fig. 9 is shown the catalytic behaviour of these materials in naphtha steam reforming process. NiMgAl sample is the most active in all range of temperatures studied; NiMgLa and NiMgCr samples present similar catalytic behaviour; whereas NiMgFe and NiMgCe samples are the most resistant to carbon deposition in spite of being less active in the studied process. Samples NiMgLa and NiMgCr present greater catalytic activity by nickel active area than NiMgAl; actually we are preparing several modifications of these materials in order to explain the catalytic behaviour. In literature [35] the promotion effect for cerium has been studied. Cerium is a promoter introduced for improving carbon resistance, and its redox properties are responsible for this behaviour.

4. Conclusions

Catalysts obtained by calcination/reduction of LDH-type materials characterized by highly dispersed metallic crystallites stabilized inside a matrix with high surface area, are suitable materials in naphtha steam reforming reaction.

The composition of the material presents an important influence on catalytic activity and carbon deposition resistance. The introduction of other elements in the structure can affect the morphology of metallic particles (dispersion, form, size and proportion of different metallic planes) of active species, and also can influence its electronic configuration modifying its reducibility and influencing interaction between adsorbed species [33]. This phenomenon produces changes in the reactivity and on catalytic behaviour.

The dispersion of the metal (and therefore the size and geometry of particles) can be modified either through the influence that support exerts on the intrinsic metal properties or by means of alloys with other metals.

In addition to the active area, the area of the support, its capacity to adsorb water and the metal–support interface, is important to the composition of the material and the electronic modifications of the active metal produced by the introduction of other elements. Therefore, high superficial area and high metallic active area are not sufficient to correlate with catalytic

activity, and it has been shown that the composition of the surroundings of nickel also influences its intrinsic activity.

From point of view of reaction mechanism, as we have seen in this issue [34], to obtain a material which presents high catalytic activity and high resistance to carbon deposition, ideal situation would be that which combines all these variables to obtain a material with a suitable combination of textural properties (dispersion, form and metallic particle size, specific area and proportion of different superficial metallic planes) to get recombination of C_1 species with oxygen species coming from the water dissociation (reaction (10)) taking place at the same rate at which they have been formed from C–C α-scission (reaction (7)), and thus to avoid C_1 species remaining on active sites sufficient time to form coke.

Amongst studied metals Ni, Cu, Co, Ru, Pd, in materials obtained from the thermal decomposition of LDH, nickel presents greater catalytic activity in hydrocarbon steam reforming in the studied conditions. On the other hand, noble metal presence (Ru, Pd), influences the carbon deposition resistance.

In order to study the influence of other elements on nickel intrinsic activity, we have studied different nickel surroundings: MgAl, MnAl, ZnAl, CaAl, LiAl, MgFe, MgCe, MgLa and MgCr. Amongst all the introduced elements we want to emphasize that the presence of basic elements (Li) remarkably improves intrinsic activity of the catalyst and its resistance to carbon deposition.

Acknowledgements

We are thankful to the Generalitat Valenciana by its aid in the financing I + D (CTIDIB/2002/20) project. N. Morlanés thanks the Ministry of Science and Technology by the concession of a predoctoral scholarship (I3P/2001).

References

[1] A. Naidja, et al. Prog. Energy Combust. Sci. 29 (2003) 155.
[2] P. Ferreira Aparicio, M.J. Benito, Catal. Rev. 47 (2005) 491.
[3] M. Krumplet, R. Rumar, K.M. Myles, J. Power Sources 49 (1994) 37.
[4] Y.S. Seo, A. Shirley, S.T. Kolaczkowski, J. Power Sources 108 (2002) 213.
[5] Science Application International Corporation, Fuel Cell Handbook, 5th edition, 2000.
[6] J.R. Rostrup Nielsen, J. Sehested, Adv. Catal. 47 (2002) 65.
[7] J.R. Rostrup Nielsen, Stud. Surf. Sci. Catal. 139 (2001) 1.
[8] J.R. Rostrup Nielsen, J. Catal. 209 (2002) 365.
[9] J. Sehested, J.A.P. Gelten, I.N. Remediakis, H. Bengaard, J.K. Norskov, J. Catal. 223 (2004) 432.
[10] V.A. Antonuci, A.S. Arico, J. Power Sources 62 (1996) 95.
[11] K. Kaneda, et al. Catal. Surv. Jpn. 4 (2000) 31.
[12] S. Natesakhawat, Thesis, The Ohio State University, 2005.
[13] F. Cavani, F. Trifiró, A. Vaccari, Catal. Today 11 (1991) 173.
[14] A. Vaccari, Appl. Clay Sci. 14 (1999) 161.
[15] F. Basile, G. Fornasari, E. Poluzzi, A. Vaccari, Appl. Clay Sci. 13 (1998) 329.
[16] D. Tichit, B. Coq, Cattech 7 (2003) 206.
[17] M. Calatayud, A. Markovits, C. Minot, Catal. Today 89 (2004) 269.
[18] F. Melo, N. Morlanés, Catal. Today 107/108 (2005) 458.
[19] M. Markevich, R. Coll, D. Montané, Ind. Eng. Chem. Res. 40 (2001) 4757.
[20] M. Markevich, R. Coll, D. Montané, Catal. Lett. 85 (2003) 41.
[21] A. Bhattacharyya, V.W. Chang, D.J. Schumacher, Appl. Clay Sci. 13 (1998) 317.
[22] S. Eriksson, U. Nylen, S. Rojas, M. Boutonnet, Appl. Catal. A: Gen. 265 (2004) 207.
[23] A. Velty, Thesis doctoral, ‘‘Química verde: catalizadores ácidos y básicos sólidos’’, 2003.
[24] B.D. Cullity, Elements of X-ray Diffraction, Addision-Wesley, London, 1978.
[25] A. Parmaliana, F. Arena, F. Frusteri, S. Coluccia, L. Marchese, G. Martra, A.L. Chuvilin, J. Catal. 141 (1993) 34.
[26] J. Bartolomew, J. Catal. 65 (1980) 73.
[27] J. Sehested, A. Carlsson, T.V. Janssens, P.L. Hansen, A.K. Datye, J. Catal. 197 (2001) 200.
[28] C. Flego, G. Consentino, M. Tagliabue, Appl. Catal. A: Gen. 270 (2004) 113.
[29] R. Birgeja, O.D. Pavel, G. Costentin, M. Che, E. Angelescu, Appl. Catal. A: Gen. 288 (2005) 185.
[30] C. Taviot-Gueho, F. Leroux, C. Payen, J.P. Besse, Appl. Clay. Sci. 28 (2005) 111.
[31] F. Kovanda, T. Grygar, V. Dornicak, T. Rojka, P. Bezdicka, K. Jiratova, Appl. Clay Sci. 28 (2005) 121.
[32] F. Garin, Catal. Today 89 (2004) 255.
[33] N.R.E. Radwan, Appl. Catal. A: Gen. 257 (2004) 177.
[34] F. Melo, N. Morlanés, Synthesis, characterization and catalytic behaviour of NiMgAl mixed oxides as catalysts for hydrogen production by naphtha steam reforming, Catal. Today 133–135 (2008) 383.
[35] S. Kurungot, T. Yamaguchi, Catal. Lett. 92 (2004) 181–187.